Optical fiber sensor determination of the water salinity based on surface plasmon resonance

Xing Liyun[1,2], Zheng Yan[1], Sun Yufeng[1], Wang Min[1], Cui Hongliang[1], Li Tingting[1]

(1. College of Instrumentation & Electrical Engineering, Jilin University, Changchun 130022, China;
2. College of Electrical and Information Engineering, Beihua University, Jilin 132013, China)

Abstract: In this thesis, the detail design of the system was discussed, including inspection system and the surface plasmon resonance (SPR) sensors based on taper technology. An Optical Fiber Sensor comparison scheme based on SPR detection of measuring the salinity of water sample was formulated to meet some practice requirements,such as accuracy, fast, small size and high sensitivity RIU (Refractive index units). The influence of each parameter on the optical fiber SPR sensor system design was simulated by using Matlab and C++, which gave a theoretical base for the choice of suitable parameters in device design. Then a new detection system, combing with optics, mechanism and electronic technology, was designed. According to the taper technology and mode field analysis theory, result of preliminary experiment shows that this device is basically met the design requirements such as compact, portable, good linearity and highly RIU. SPR experiments about NACL-water mixture with different salinity are implemented in this new device, and experimental results show that accurate detection on single sample can be achieved, and the detecting of the resonance wavelength differentiation is 0.15 nm, moreover, the detecting results has high linearity and good stability, and the refraction index(RI) detecting deviation is less than 0.002.

Key words: taper optical fiber sensor; SPR; salinity; RUI; linearity

CLC number: O799 **Document code:** A **Article ID:** 1007-2276(2015)04-1290-07

基于光纤SPR传感器水中盐度的测定

邢砾云[1,2],郑 妍[1],孙玉锋[1],王 敏[1],崔洪亮[1],李婷婷[1]

(1. 吉林大学 仪器科学与电气工程学院,吉林 长春 130022;
2. 北华大学 电气信息工程学院, 吉林 吉林 132013)

摘 要: 论述了检测系统和基于拉锥技术的光纤表面等离子共振(SPR)传感器的详细设计。制定了基于SPR的光纤传感器检测水样品的盐度的比较方案,以满足一些实践需求,诸如精度,速度快,小尺寸和高灵敏度折射率单位(RIU)。利用Matlab和C++仿真得到了每个参数对光纤拉锥SPR传感器系统设计性能的影响,这为设备参数的合理选择提供了理论依据。设计了一种新的检测系统,将光学、机械和电子技术相结合。根据拉锥技术、模场分析理论及初步实验结果表明,该装置基本上达到了设计要求,如小巧、便携、良好的线性度和高度单位折射率。基于这个新设备对具有不同的盐度的NACL-水混合

收稿日期: 2014-08-05; **修订日期:** 2014-09-13

基金项目: 国家自然科学基金面上项目(41376185);国家海洋局项目(201405026-01)

作者简介: 邢砾云(1981-), 女 ,讲师,博士,主要从事太赫兹无损检测技术、太赫兹光谱及成像技术、表面等离子共振方面的研究。
Email:xingliyun116@foxmail.com

物进行了 SPR 实验，实验结果表明，可以实现对单个样品的精确检测。其谐振波长分辨率可以达到 0.15 nm，同时，该检测结果具有较高的线性度和良好的稳定性，折射率(RI)检测偏差小于 0.002。

关键词：光纤拉锥传感器；　表面等离子共振；　盐度；　单位折射率；　线性度

0 Introduction

Currently, fast and high -precision biomedical detection has been broadly applied in basic biology research, clinic test and other areas. However, preexisting instrumentation are too huge and expensive for promotion. Surface plasmon resonance(SPR) sensor is one of the latest inspection method based on physical optics. Its characteristics include but not limited to high sensitivity, fast inspection, low sample consumption, no label and zero damage, so it has been widely used in surface inspection, biomedical (biochemical) analysis, drug screening, environment monitoring, and so on.

So far, as an important technology to study interactions between biological macromolecules, it has obtained wide attention from domestic and international scientists.

Commonly，there are three kinds of main excitation methods to realize SPR, which are the prism type, fiber type and grating structure. From the points of quality factor and monitoring RI range, the detection of prism effect is best. From the points of equipment miniaturization and remote monitoring, optical fiber type has certain advantages. Grating structure on the implementation structure is relatively complex, the study of different structure can realize the sensitivity and accuracy of different requirements[1-2].

Sell on the market at presen most of the SPR detector based on the Kretshmann theory, monitoring scope generally between 1.33 -1.40, this range is limited. On the design of the instrument of optical fiber in favor of the miniaturization of the equipment as well as the needs of remote on-line detection. In recent years, in order to improve the practical application of SPR technology, the research of optical fiber SPR become a hot spot[3-4], mainly including the structure of the SPR sensor probe such as fiber optic polishing, taper; the structure of the fiber optic micro machining; metal film surface structures and composite materials research; sensing structure such as the structure of FP cavity and Raman enhanced surface plasma resonance, etc[5].

The development direction of SPR application technology in the future, mainly includes the detection range of flexible, equipment miniaturization, improving the accuracy, and the detection results′ linearity and stability.

1 Theoretical analyses

1.1 Fiber optic tapering theory

Fused t aper fiber is to put the stripped naked optical fiber on the high temperature to heat, and then pulling the fiber core and cladding while fine (as shown in Fig.1). Fiber optic taper technology, including fixed and mobile fire flame tapering. Among them, the mobile fire flame is the primary method of making a controlled precise shape tapering fiberand accurate shape.

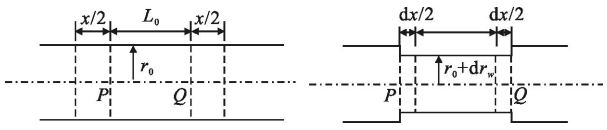

(a) Fiber before being tapered (b) Fiber after flame scanning once

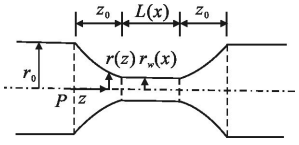

(c) Fiber after being tapered

Fig.1 Schematic diagram of a tapered fiber[6]

According to the fiber before tapering volume

should satisfy conservation relations. Namely, fiber is stretched partial volume remains unchanged shows that[4]:

$$\pi(r_w+\mathrm{d}r_w)^2(L+\mathrm{d}x)=\pi r_w^2 L \tag{1}$$

To ignore the higher order infinitesimal, it can deduce that[6]

$$\frac{\mathrm{d}r_w}{r_w}=-\frac{\mathrm{d}x}{2L(x)} \tag{2}$$

Considering the fiber tapered length changing from 0 to x, the corresponding radius transforming from r_0 to r_w[7],

$$\int_0^{r_w}\frac{\mathrm{d}r_w}{r_w}=-\int_0^{x}\frac{\mathrm{d}x}{2L(x)} \tag{3}$$

So that

$$r_w(x)=r_0\exp\left[-\int_0^{x}\frac{\mathrm{d}x}{2L(x)}\right] \tag{4}$$

So, the rule of each flame scanning scope $L(x)$ can be accorded to work out the ultimate values in different tapered distance corresponding to the waist radius of the fiber. We can see from Fig.1:

$$2z_0+L(x)=x+L_0 \tag{5}$$

Sothe relationship between the tapered distance and deformation zone length is showed:

$$x=2z_0+L(x)-L_0 \tag{6}$$

It can see from Fig.1(c), in the process of pulling taper, waist area starting point (that is the end of the conical) coordinates is z_0, relationship between x and z, shape function in the taper fiber deformation zone are obtained[6]:

$$r(z)=r_w(x(z)) \tag{7}$$

If the flame scanning range is fixed or the width is invariable,

$$L(x)=L_0 \tag{8}$$

So that

$$r_w(x)=r_0\exp(-x/2L_0)\quad x=2z \tag{9}$$

Then the deformation zone function can be gotten as follows[6]:

$$r(z)=r_0\exp(-z/L_0) \tag{10}$$

It is an exponential decay model tapered function. Where, each physical unit is μm. The waist length of the tapering fiber is the width of the fixed or fixed flame moving range.

Fiber optic probe geometry is represented by Taper Ratio (TR), the expression is:

$$P_{\mathrm{TR}}=\frac{r_w}{r_0} \tag{11}$$

1.2 Theory of optical fiber taper and the of relationship transmission power

To illustrate the relationship about the transmission loss with the test solution RI changes, create the following simple model: the original fused taper fiber core cladding layer and is equivalent to the new model, and the test solution as a new packet-layer model. The new core RI is equivalent to the effective RIn_{eff} of the tapered fiber core; the new cladding RIn_0 is the RI of the test solution. In order to understand that when the variation of the new cladding RI, how the power in the total power ratio carried by the core changes, it is with the LP_0 mode as a case.

LP_0 mode field distribution is similar to a Gaussian distribution, can be approximated by a Gaussian function instead of the exact field expressions. Thus, the ratio of the total optical power carried by the power of the new core is as follows[3]:

$$\frac{P_C}{P_T}\approx 1-\exp\left[-2\left(\frac{r_w}{S_0}\right)^2\right] \tag{12}$$

Let P_C and P_T denote the power carried by the core and the total power, respectively, r_w denote the new core radius, S_0 denote the new mode field radius (MFR).

Then the tip radius varies with the coordinate z according to[8]

$$r(z)=r_0-\left[\frac{z}{L}(r_0-r_w)\right] \tag{13}$$

In the tapered region, the angle range of the rays at the coordinate z alters to $[\varphi_1(z),\varphi_2(z)]$ due to the variation of fiber core diameter, where

$$\varphi_1(z)=a\cos\left(\frac{r_0\cos\theta_{cr}}{r(z)}\right)-\Omega \tag{14}$$

$$\varphi_2(z)=\frac{\pi}{2}-\Omega \tag{15}$$

$\Omega=a\tan[(r_0-r_w)/L]$ is taper angle, $\theta_{cr}=a\sin(n_{c1}/n_1)$ is criticalangle, n_{c1} is the RI of the cladding.

Especially, when $r_0=r_w$, the SPR-based optical fiber tip returns to the SPR-based cylinder fiber tip.

As shown in Fig.1, the excitation light from a collimated source is launched into one end of the fiber at the axial point, the normalized reflecting power of p-polarized light can be written as[1-2,5-6]:

$$P_{\text{reff}}=\frac{\int_0^L \mathrm{d}z \int_{\varphi_1(z)}^{\varphi_2} R_P^{2N_{\text{ref}}(\theta,z)} P(\theta)\mathrm{d}\theta}{\int_0^L \mathrm{d}z \int_{\varphi_1(z)}^{\varphi_2} P(\theta)\mathrm{d}\theta} \tag{16}$$

Where

$$P(\theta)=\frac{n_1^2 \sin\theta\cos\theta}{(1-n_1^2\cos^2\theta)^2} \tag{17}$$

$$N_{\text{ref}}(\theta,z)=\frac{L}{2r(z)\tan(\theta-\Omega)} \tag{18}$$

And R_p is the amplitude reflection coefficient for p-polarized incident wave.

2 Detailed design of the SPR system

A new RI fiber optic sensor with low cost, easy operation and the capability of multipoint parallel measurement is explored. A putter is used in the fiber optic sensor RI to achieve multipoint parallel measurement. A high stable amplified spontaneous emission light source and three optical power meters are used as broadband source and detectors, respectively.

2.1 Preparation of the sensing probe

In order to increase the role of the length of the sensing area, to further improve the sensitivity of the sensor, a reflective element was accessed at the output of the sensor head fused taper fiber. After the light is reflected by the optical fiber sensor head output sensing area again, then return to the original fiber, which was finally received by the photodetector. It is worth emphasizing that the introduction of the reflective element may be not only the sensing area of the sensor length is doubled and enhanced, it can make a photodetector in the transmitter of the sensor system, remote monitoring, and can also take advantage of multi-point real-time spectra l sensing and measurement in parallel. Figure 2 shows SPR probe prepared tapering structure and physical figure.

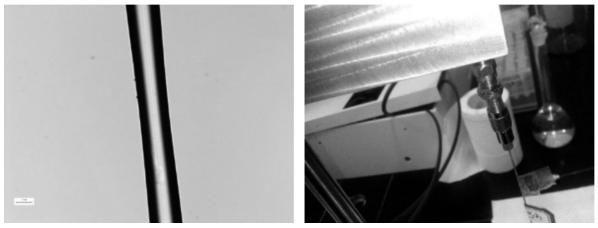

(a) Tapered fibers observed under the microscope　(b) Tapered fibers physical figure

Fig.2 SPR probe prepared tapering structure and physical figure

2.2 Experimental setup

In this paper, fiber optic SPR sensor system consists of a broadband light source, SPR sensing probes, multi-mode fiber coupling device, miniature fiber optic spectrometers and computer components, shown in Fig.3. Incident light is generated by a broadband light source, a total disaster by multimode fiber into the SPR sensing probe, the light emitted from the SPR sensing probe through the other end of the coupling device into the spectrometer for changes in reflectance spectra collected.

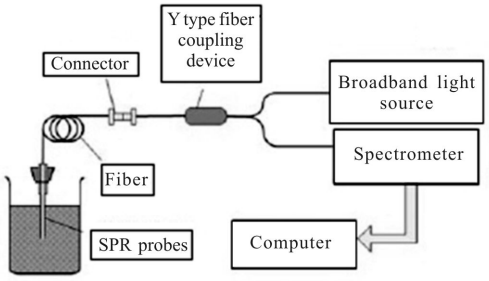

Fig.3 Fiber optic SPR sensor system structure

The experimental setup for characterizing the SPR fiber optic sensor is shown in Fig.3. Unpolarized light from a tungsten halogen lamp (HL-2000-HP, Ocean Optics) was coupled to the fiber optic SPR probe though a Y type fiber coupler. The SPR probe was fixed in a glass flow cell to allow the liquid samples to flow and encircle the probe. The effected spectrum was captured by a fiber optic spectrometer (HR4000, Ocean Optics, the detecting of the resonance wavelength differentiation is 0.15 nm), which was connected to the other side of the coupler. The spectra

were recorded and analyzed by program written in C ++ and MATLAB. An Abbes´ refract meter (Shanghai Optical Instrument Plant) was used to measure the RI of the solutions.

3 MATLAB simulation

Making use of MATLAB software, computer simulation studies are made to validate of the design parameters influence on the optical fiber SPR sensor system.

According to the formula (16), we can simulate the light emission spectrum (light intensity transmittance curve) which passed the sensing region to obtain a resonance peak of the SPR sensor (light intensity transmittance curve minimum value) and then come to the sensitivity and detection accuracy of the sensor. Sensitivity and detection accuracy of the sensor are two important parameters to measure the performance of fiber optic SPR sensor. The higher the value of these two parameters the better performance of the sensor. SPR sensor sensitivity depends on the displacement of the resonance peak when the RI of the surrounding medium changes. When measured RI change, the displacement of formant SPR. The RIU sensitivity is defined as[6]

$$S_n=\frac{\delta\lambda_{res}}{\delta n_s} \tag{19}$$

Where δn_s is the change in RI of solution and $\delta\lambda_{res}$ is the corresponding resonance wavelength shift.

A simple model is established, and the relation between the ratio of the light power carried by the core versus the total light power of a fiber and the external RI is analyzed in detail. In the simulation, the transmittance of sample solution with different RI are calculated, the calibration curve between Taper Ratio (TR) and RI unit (RIU) by comparison is obtained. It is found that the TR value will influence the RIU and detection accuracy. The simulation verifies that it can improve the system sensitivity greatly by introducing a tapered fiber probe[8-10].

In this paper, the metal film is directly in contact with the sample, such sensor without sensing layer may be considered as a case of $d3$=0. In addition, the parameters of optical fiber (n_1=1.457, n_{cl}=1.450, n_{ref}=1.46, r_0=600μm), and Au film with the thickness of $d2$=50nm are fixed.

3.1 TR impact on the SPR characteristics(omega)

With the absorption ratio of peak broadening, TR from 1 to 2.6 with 0.08 intervals simulation analysis shows that the value from 1 to 1.64, the sensor has a high accuracy. The simulation results was shown as Fig.4 to Fig.6

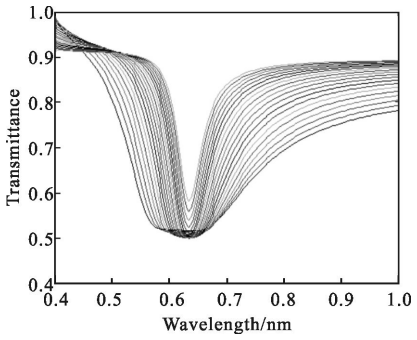

Fig.4 Different TR and energy transmittance curve

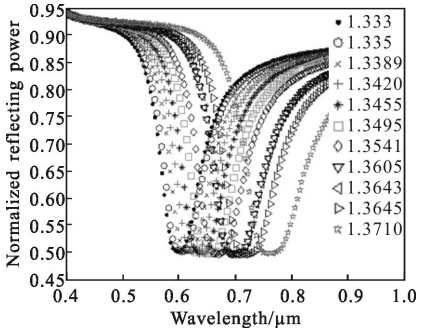

(a) Untapered RIU=4210.1(nm/RI)

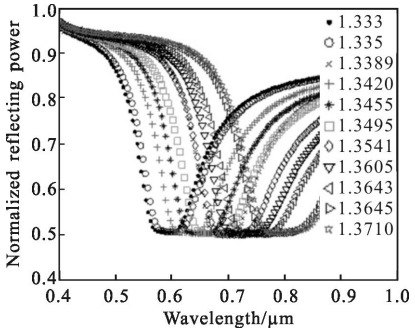

(b) Tapered RIU=5997.8(nm/RI) (TR=1.8)

Fig.5 Simulation RIU contrast

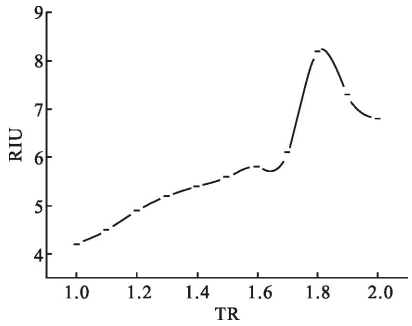

Fig.6 Relationship between sensitivity (μm/RIU) of the SPR fiber optic sensor and TR

4 Experimental results and analysis

Fig.7(a) shows the plots of resonance wavelength shift with the change of refractive index of NACL–water mixture observed from untapered sensors. Fig.7(b) shows typical reflectance spectra of SPR sensor with 10 mm tapered sensor length when it was exposed to NACL–water mixture with different salinity, corresponding to the RI varying in the range of 1.333 –1.3710 (as shown in Tab.1). As shown in Fig.7 (b), there is a clear SPR wavelength redshift with the increase of the RI of the solution.

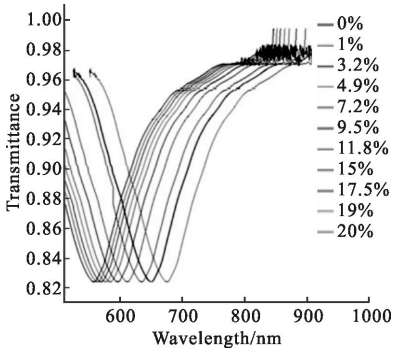

(a) Untapered RIU=3015.1(nm/RI)

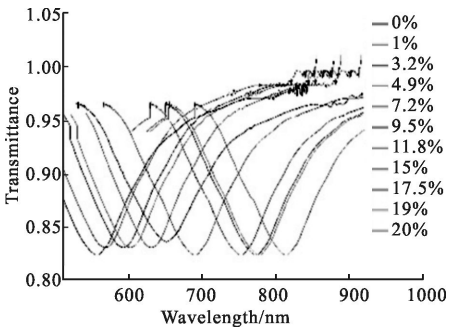

(b) Tapered RIU=5997.8(nm/RI) (TR=1.6)

Fig.7 Experimental RIU contrast, concentration percentage curve is increased in order, from left to right

Tab.1 Relation between the salinity and RI of NACL solution

Salinity	RI
0	1.333
1	1.335
3.2	1.338 9
4.9	1.342 0
7.2	1.345 5
9.5	1.349 5
11.5	1.354 1
15	1.360 5
17.5	1.364 3
19	1.364 5
20	1.371 0

4.1 Contrast sensitivity tapering experimental data

The refraction index (RI) detecting deviation is less than 0.002.

4.2 Tapering linearity comparison of experimental data

The response of all three SPR sensors is non–linear and can be regarded as a function of RI. But the tapered fiber sensor is better than untapered apparently, as Fig.8 shown.

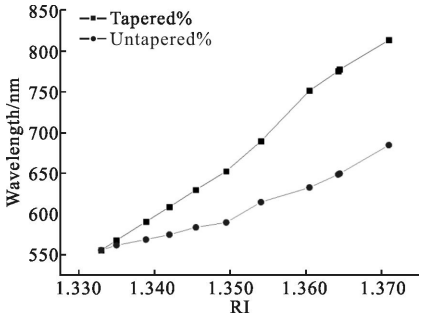

Fig.8 Linearity comparison

5 Conclusion

By com paring the simulation, the test of the NACL solution of different concentrations with different RI, we can see tapering detector can significantly improve the RI sensitivity and linearity. It shows that with the increase of the TR, the sensitivity

increases and the accuracy reduces. Considering the two indicators, the sensor has a good performance when TR is between 1.2 –1.64. Based on the theoretical simulation result, the tapered probe is fabricated and the experimental system is set up. Before tapering, the experimental results due to the influence coating quality and accuracy, accuracy of detection accuracy only reached 3.105 μm/RIU. The tapered results show that the sensitivity of the sensor is 5.99 μm/RIU, which is well consistent with the result of theoretical simulation (5.90 μm/RIU). And the tapered fiber sensor is better than untapered.

References:

[1] Jin Fengze, Du Chunlei1, Shi Lifang, et al. Experimental study of surface plasmon wave imaging sensors [J]. ***Infrared and Laser Engineering***, 2010, 39(2): 275–278. (in Chinese)

[2] Gupta B D, Sharma A K. Sensitivity evaluation of a multi-layered surface plasmon resonance-based fiber optic sensor: a theoretical study [J]. ***Sensors and Actuators B***, 2005, 107: 40–46.

[3] Yu Huang, Wei Zhang, Wanyi Xie, et al. Influence of ions on dynamic response of surface plasmon resonance fiber optic sensor[J]. ***Sensors and Actuators B***, 2013, 186: 199–204.

[4] Jimenez Rioboo R J, Philipp M, Ramos M, et al. Concentration and temperature dependence of the refractive index of ethanol-water mixtures: influence of intermolecular interactions [J]. ***European Physical Journal E: Soft Matter and Biological Physics***, 2009, 30: 19–26.

[5] Sharma A K, Gupta B D. Comparison of performance parameters of conventional and nano-plasmonic fiber optic sensors[J]. ***Plasmonics***, 2007, 2: 51–54.

[6] Sun Weimin, Shi Shuai, Dai Qiang. Fabrication and measurement of tapered fiber[J]. ***Journal of Optoelectronics·Laser***, 2009, 20(11): 1474–1477.

[7] Dwivedi Y S, Sharma A K, Gupta B D. Influence of design parameters on the performance of a surface plasmon sensor based fiber optic sensor[J]. ***Plasmonics***, 2008, 3: 79–86.

[8] Suzuki H, Sugimoto M, Matsui Y, et al. Effects of gold film thickness on spectrum profile and sensitivity of a multimode-optical-fiber SPR sensor[J]. ***Sensors and Actuators B***, 2008, 132: 26–33.

[9] Yuan Y, Wang L, Huang J. Theoretical investigation for two cascaded SPR fiber optic sensors [J]. ***Sensors and Actuators B***, 2012, 161: 269–273.

[10] Yuan Yinquan, Hu Die, Hua Li, et al. Theoretical investigations for surface plasmon resonance based optical fiber tip sensor [J]. ***Sensors and Actuators B***, 2013, 188: 757–760.